



# Investigations on Copper Cast Cakes, Sickle Fragments and a Spout Axe of the Hoard Find from Drassburg/Burgenland

Roland Haubner<sup>1</sup> · Susanne Strobl<sup>1</sup>

Received: 12 September 2022 / Revised: 10 January 2023 / Accepted: 24 January 2023 / Published online: 24 February 2023  
© The Author(s) 2023

## Abstract

The Bronze Age hoard from Drassburg contains among other objects cast cakes, sickles, spout axes and fragments of these. Ten copper alloy samples were examined by metallography. The high Pb content of three cast cakes indicates that Pb or Pb ores were intentionally added to the metallic copper. Two cast cakes contain small amounts of Pb and probably copper from the primary production. One cast cake is a Sn bronze. The sickle and socket axe fragments are Sn bronze with different composition. Most microstructures show dendritic solidification, and sometimes, deformation structures are observed. It can be assumed that the copper alloys of the Drassburg hoard were used for recycling. If one considers the quite different alloy compositions, it is impossible to trace the copper ore sources using Pb isotopy or trace element analysis. This applies to the present copper alloys as well as to objects made from recycled material.

**Keywords** Bronze Age · Copper hoard · Cast cake · Sickle · Socket axe

## Introduction

### The Drassburg Hoard and the Examined Copper Objects

In 1932, a bronze depot was found in a vineyard near Drassburg in Burgenland which contains copper objects with 25 kg total weight. In addition to copper cast cake fragments, this hoard includes sickles, sickle fragments, other tools like socket axes and lots of jewellery in various states of preservation [1]. A compilation of the hoard and a detailed description or material analyses are not known. The Drassburg bronze depot is comparable to hoard finds

from the Urnfield period [2]. Since Burgenland geographically belongs to the Pannonian lowlands, a corresponding chronology of the Bronze Age is attached [3].

### Bronze Age Hoards

Hoards or depots are an important source of archaeological finds. According to the classical definition, a hoard consists of several archaeological objects found in close proximity. It is assumed that these objects were stored intentionally. They were, for example, sacrificial or votive offerings, raw material stores for traders or bronze foundries or hiding places for treasure deposits in times of crisis. Thus, offerings in water or moors are sacred, irreversible deposits, but raw material deposits in the ground are profane and reversible [4–6].

Therefore, a hoard of broken bronze objects, bronze ingots and bronze cast cakes can be interpreted as a bronze material craftsman's store. A depot of aesthetic bronze objects is rather associated with a merchant or could have been placed as a votive offering [3].

Numerous bronze hoard objects of various compositions have already been found in Europe [7–13].

---

This invited article is part of a special topical issue of the journal *Metallography, Microstructure, and Analysis* on Archaeometallurgy. The issue was organized by Dr. Patricia Carrizo, National Technological University—Mendoza Regional, and Dr. Omid Oudbashi, Art University of Isfahan and The Metropolitan Museum of Art, on behalf of the ASM International Archaeometallurgy Committee.

---

✉ Roland Haubner  
roland.haubner@tuwien.ac.at

<sup>1</sup> Institut für Chemische Technologien und Analytik,  
Technische Universität Wien, Getreidemarkt 9/164-CT,  
1060 Vienna, Austria



**Fig. 1** Copper cast cakes (cc) from Drassburg. Whole cast cake **a** top, **b** bottom, **c** cast cake with a smooth surface from splitting, (**a–c**) not examined. Examined cast cakes **d** cc1, **e** cc2, **f** cc3, **g** cc4, **h** cc5, **i** cc6.

### Copper Metallurgy, Copper Casting Cakes and Recycled Material

The metallurgy of copper started with the production of almost pure copper followed by copper arsenic, arsenic bronze and finally tin bronze was produced [14–17]. The impurities in the smelted copper depend on the composition of the used ore (malachite, fahlore or chalcopyrite) and the metallurgical processes [18–21]. For example, by smelting fahlores small amounts of As and Sb are detected in the copper [22, 23].

Since copper ores are usually not associated with lead ores and there are usually no high concentrations of Pb in the copper ingots, the metallurgists of the time may have already experimented with the use of additives [24, 25]. For example, studies showed that antimonite ( $\text{Sb}_2\text{S}_3$ ) was added to copper. Something similar would be possible with galena (PbS). It is described that the extraction of metallic lead was already known in the Bronze Age, but there are no corresponding archaeological finds.

With the development of tin bronzes by adding deliberately cassiterite ( $\text{SnO}_2$ ) or metallic Sn to the copper, additional impurities from cassiterite were introduced into the bronze [26, 27].

**Table 1** XRF data measured in wt% on the metallographic prepared samples (ldl = lower detection limit)

wt. % element	casting cakes						sickles			socket axe
	cc 1	cc 2	cc 3	cc 4	cc 5	cc 6	si 1	si 2	si 3	sa 1
<b>Cu</b>	<b>81,36</b>	<b>91,45</b>	<b>70,84</b>	<b>84,47</b>	<b>96,74</b>	<b>99</b>	<b>94,49</b>	<b>87,92</b>	<b>92,26</b>	<b>92,5</b>
Sn	0,16	0,78	5,13	14,41	ldl	ldl	4,31	10,06	6,49	4,47
Pb	<b>17,32</b>	<b>7,35</b>	<b>23,43</b>	0,75	0,07	0,32	0,61	0,79	0,7	<b>2,54</b>
As	ldl	0,12	0,09	ldl	<b>1,08</b>	ldl	0,14	0,15	ldl	0,14
Bi	0,08	ldl	ldl	ldl	ldl	ldl	ldl	ldl	0,09	0,09
Zn	0,07	ldl	ldl	ldl	ldl	ldl	ldl	ldl	ldl	ldl
Ni	ldl	0,2	0,25	0,21	0,59	ldl	0,2	0,24	0,22	0,18
Co	0,16	n.n.	0,06	ldl	0,35	ldl	0,07	ldl	ldl	ldl
Fe	0,24	n.n.	ldl	ldl	0,62	0,17	0,06	0,43	ldl	ldl
<b>S</b>	<b>0,63</b>	0,09	<b>0,2</b>	<b>0,16</b>	<b>0,55</b>	<b>0,51</b>	<b>0,12</b>	<b>0,31</b>	<b>0,24</b>	0,08
Si	ldl	ldl	ldl	ldl	ldl	ldl	ldl	0,09	ldl	ldl

The coloured numbers are intended to draw attention to particularly high measured values of the respective element

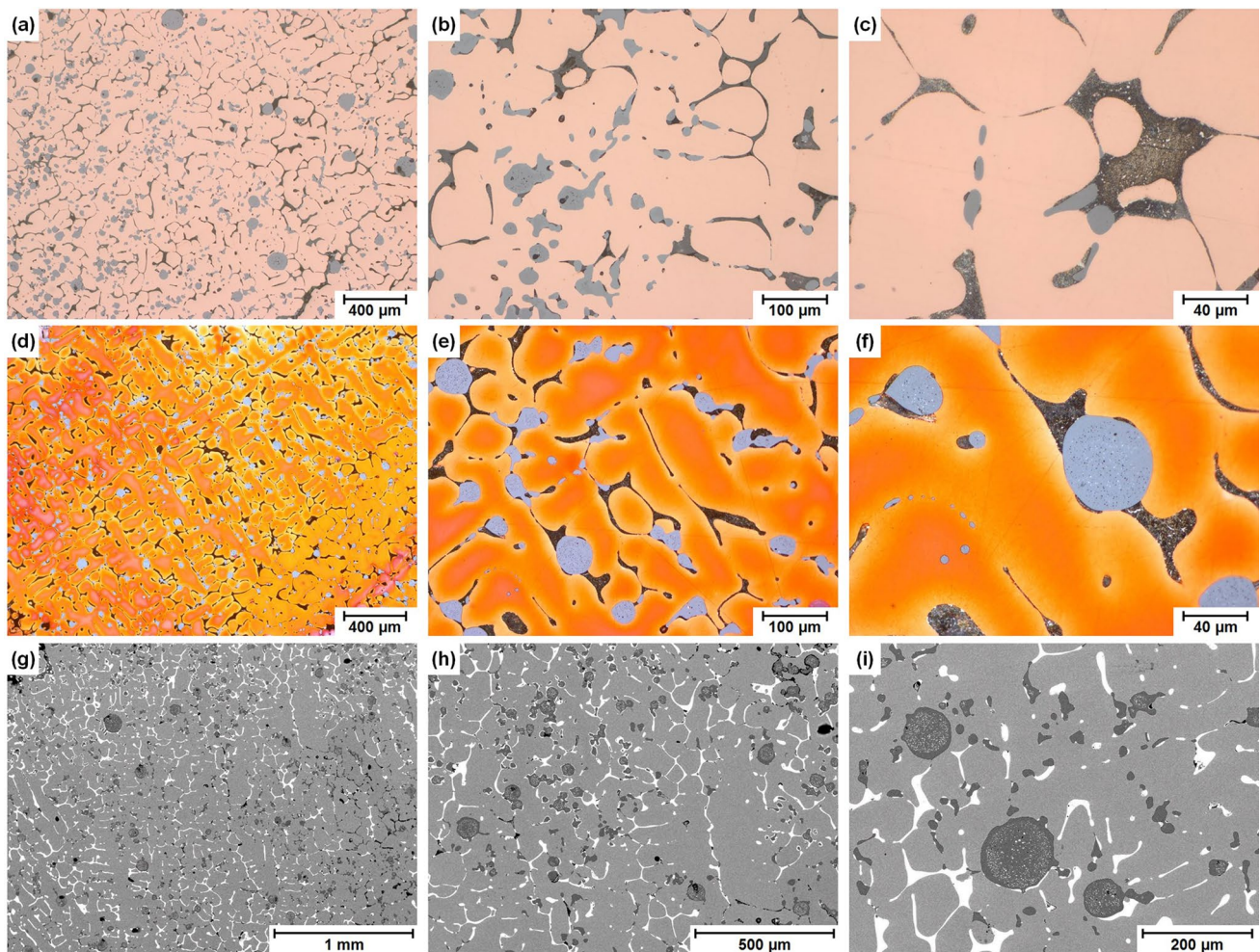


**Fig. 2** Metallography of cast cake cc1. **a–c** Polished sample, LOM, **d–f** Klemm2 etched, LOM, **g–i** SEM.

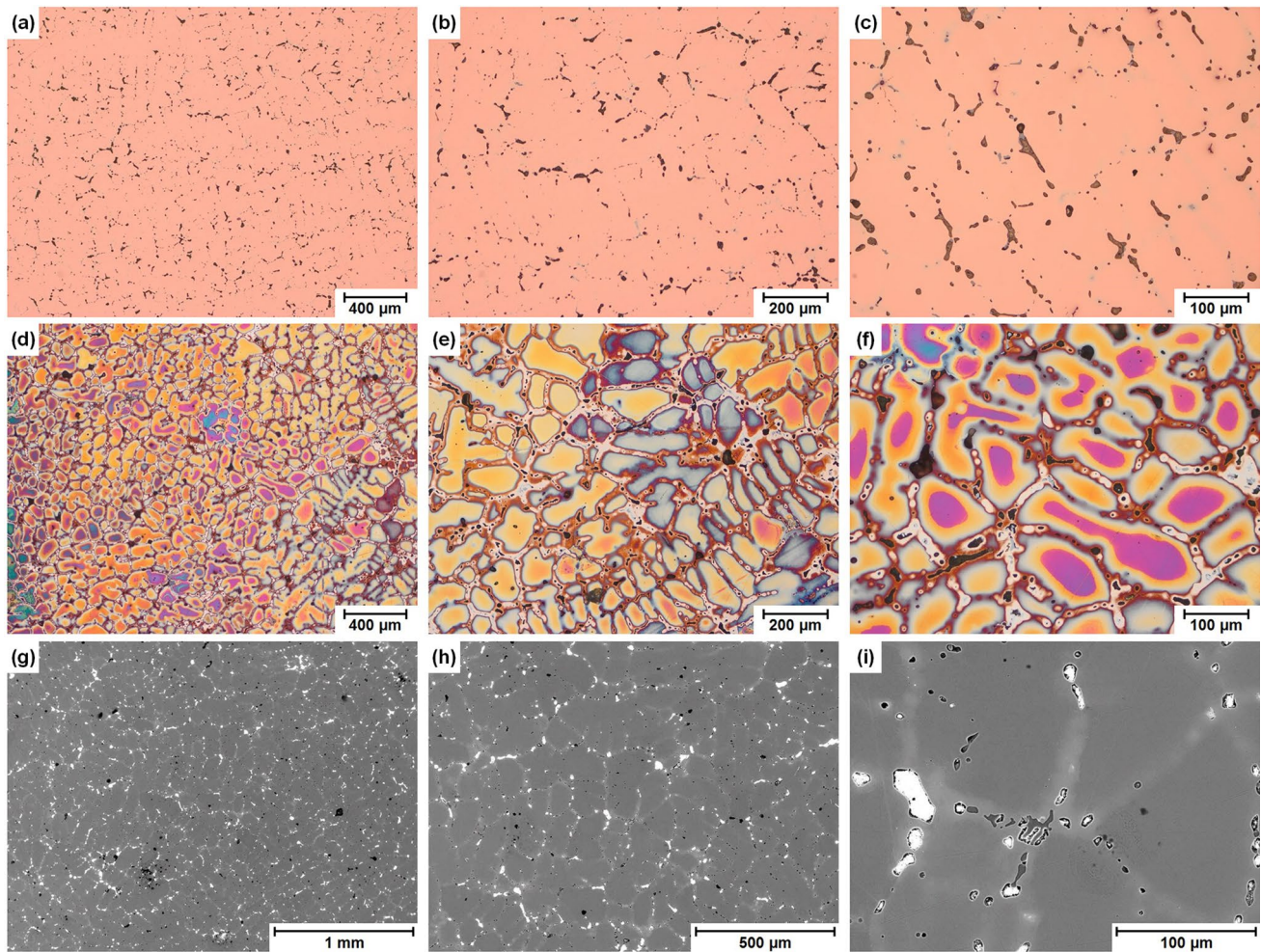


**Fig. 3** Metallography of cast cake cc2. **a–c** Polished sample, LOM, **d–f** Klemm2 etched, LOM, **g–i** SEM1

Last but not least, copper ingots made from recycled material should be mentioned. All impurities can be present in a broad variation of concentrations in this Cu. The different copper objects in a hoard suggest that the various alloys were mixed by recycling.

Figure 1 shows a compilation of various hoard finds.

## Experimental Procedures

Six fragments of copper cast cakes “cc”, three bronze sickle fragments “si” and one spout axe “sa” fragment were made available for metallographic investigations. From all samples, small pieces were sectioned using a metallographic cutting machine. The specimens were cold-mounted and

metallographically prepared. Klemm2 solution was used as etchant. Light microscope (LOM) and scanning electron microscope (SEM) with energy-dispersive X-ray (EDX) analysis were used for the investigations as well as X-ray fluorescence (XRF) analysis for an average analysis.

## Results and Discussion

To determine the chemical composition, XRF analyses were carried out at the metallographically prepared cross sections of the bronze specimens. The results are summarized in Table 1. Surprisingly, Pb contents between 7 and 24% by weight were detected in three casting cakes and two samples contained more than 5% by weight Sn. The sickle fragments

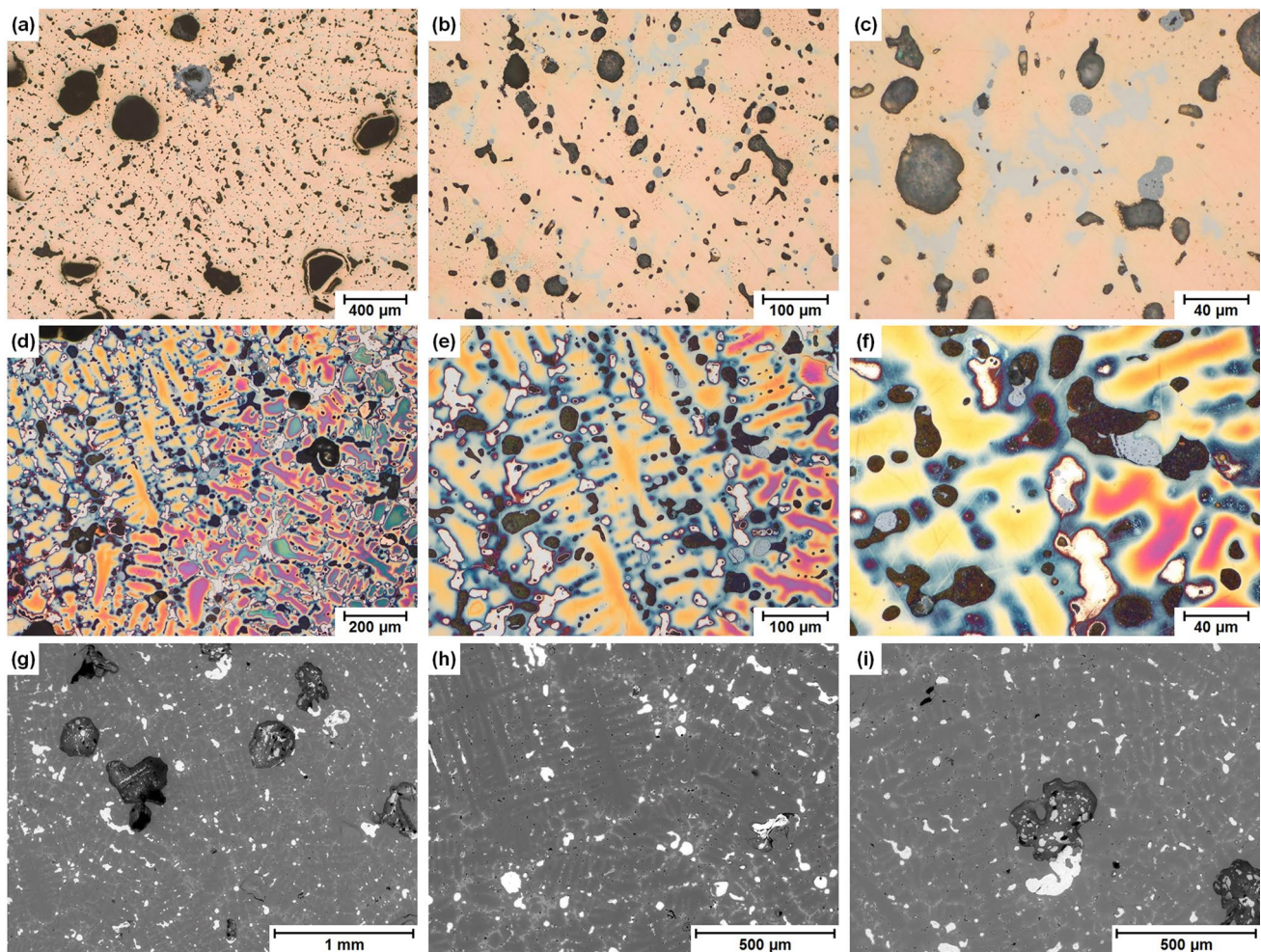


**Fig. 4** Metallography of cast cake cc3. **a–c** Polished sample, LOM, **d–f** Klemm2 etched, LOM, **g–i** SEM.

and the socket axe consisted of Sn bronze with different Sn contents. Further results follow in the description of the individual samples.

### The Copper Cast Cakes

The copper cast cake cc1 contains 17.32 wt% Pb, 0.63 wt% S, small amounts of Sn and Fe as well as some other impurities (Table 1). In the metallographic section, one can see a very coarse dendritic copper structure, whereby the typical branching of the dendrites is hardly visible (Fig. 2a–c). After etching the sample, an orange colour can be seen inside the copper dendrite, which becomes lighter towards the edge (Fig. 2d–f). This can be explained by segregation effects, since during progressive solidification more impurities are incorporated into copper. In the interdendritic areas, Pb

appears dark grey (Fig. 2a–c). Due to the low melting point of Pb, it solidifies at last. After etching, Pb appears almost black (Fig. 2d–f), but in SEM-BSE Pb is white (Fig. 2g–i). Spherical precipitations of  $\text{Cu}_2\text{S}$ , with a diameter of up to 50  $\mu\text{m}$ , can be seen in the structure (Fig. 2a–c). After etching,  $\text{Cu}_2\text{S}$  is light grey (Fig. 2e, f), but in SEM-BSE it is dark grey (Fig. 2h, i).

cc2 contains 7.35 wt% Pb, 0.78 wt% Sn, 0.12 wt% As and only 0.09 wt% S (Table 1). The microstructure is dendritic (Fig. 3a–c) and the interdendritic areas are significantly smaller than in cc1. In the etched state, the inner areas of the dendrites are coloured dark red and a colour gradient is clearly distinguishable. This can be explained by the presence of Sn. In SEM, the interdendritic areas with Sn enrichment are light grey and Pb is white.

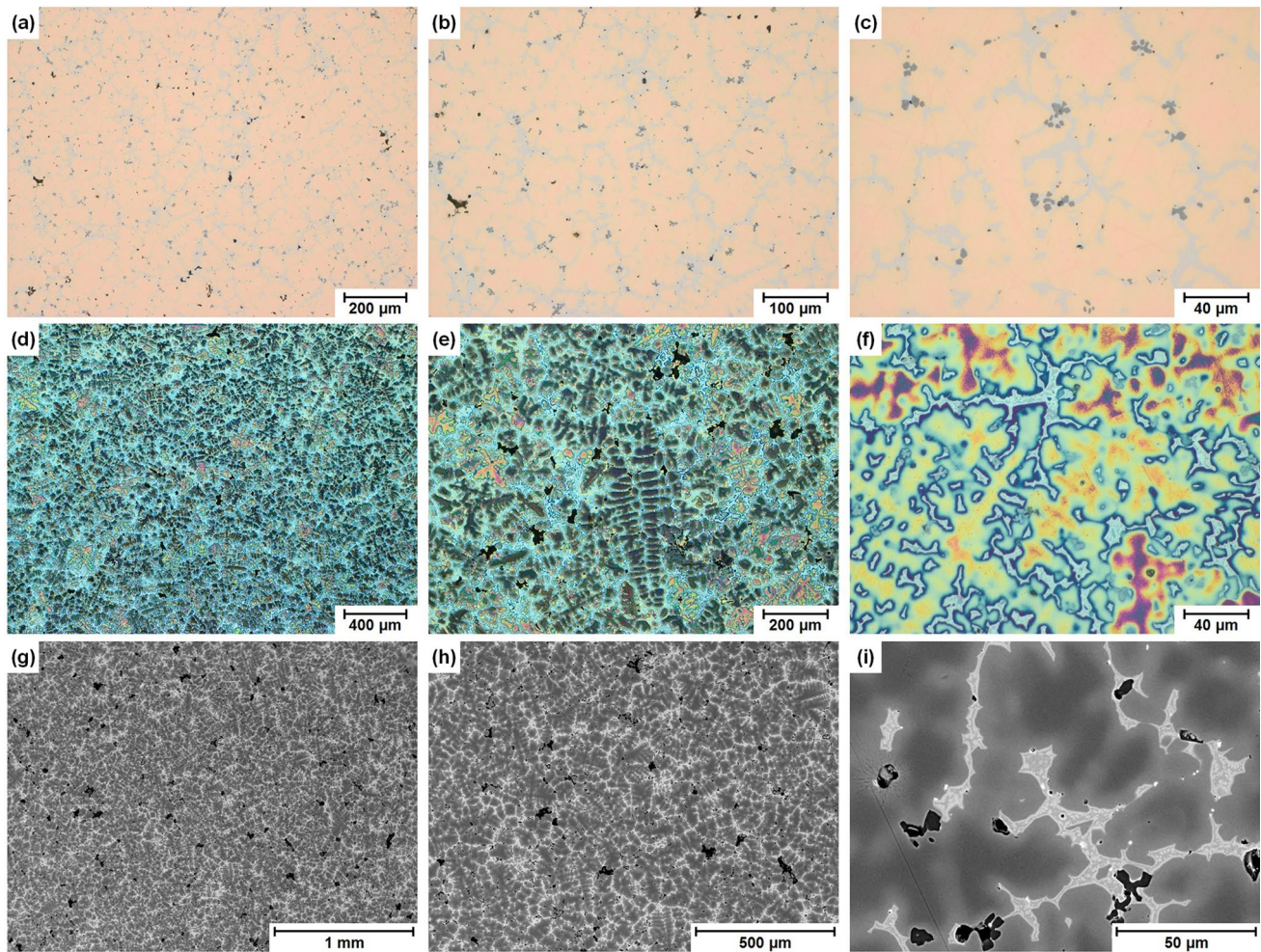


**Fig. 5** Metallography of cast cake cc4. **a–c** Polished sample, LOM, **d–f** Klemm2 etched, LOM, **g–i** SEM.

cc3 still has a dendritic structure, but due to a high Pb and Sn content a considerable amount of interdendritic area can be observed. It contains the highest amount of Pb with 23.43 wt%, as well as 5.13 wt% Sn, 0.09 wt% As and 0.2 wt% S (Table 1). Even in the polished state, an eutectoid of light blue  $\text{Cu}_{41}\text{Sn}_{11}$  and Cu-Sn solid solution can be seen next to the dark grey Pb (Fig. 4a–c). After etching, Pb is black and the intermetallic phase  $\text{Cu}_{41}\text{Sn}_{11}$  is white. Again, a colour gradient is observed between the interior of the dendrites and the interdendritic areas (Fig. 4d–f). In SEM, the interdendritic areas with Sn enrichment are light grey and the Pb is white (Fig. 4g–i).

The casting cakes cc1, cc2 and cc3 are characterized by high Pb contents. Since the usual copper ores tend to have low amounts of Pb [28, 29], it can be assumed that Pb ores

(e.g. galena  $\text{PbS}$ ) were added to the Cu. This process has already been observed with Sb, because at that time antimonite ( $\text{Sb}_2\text{S}_3$ ) was added to the Cu. Both phases Cu-Sb and  $\text{Cu}_2\text{S}$  are formed [19].

No relevant literature was found on the reactions of PbS with molten Cu; however, it is probable that metallic Pb and  $\text{Cu}_2\text{S}$  are formed. Due to its high density, Pb should sink rapidly in Cu and  $\text{Cu}_2\text{S}$  should rise slowly, resulting in segregation. The final composition of the casting cake depends on the mixing ratios and how fast a  $\text{Cu}_2\text{S}$  slag layer on the surface is formed.

One can only speculate about the motivation to add Pb to copper, because the mechanical properties of Cu are not improved by Pb. Maybe they just wanted to increase the amount of metal.

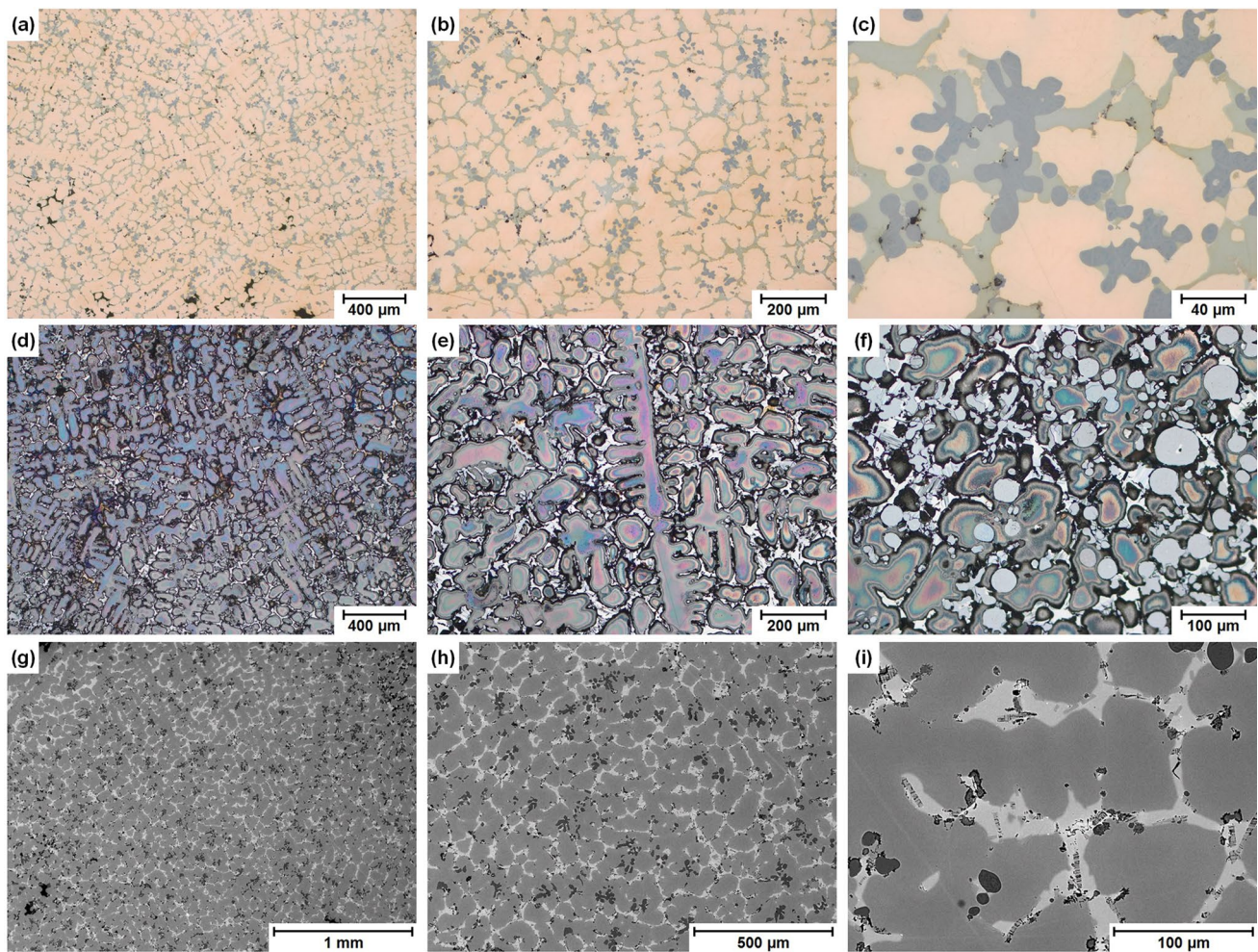


**Fig. 6** Metallography of cast cake cc5. **a–c** Polished sample, LOM, **d–f** Klemm2 etched, LOM, **g–i** SEM.

cc4 has the highest amount of Sn with 14.4 wt% as well as 0.16 wt% S and only 0.75 wt% Pb (Table 1). The cast structure is dendritic and the eutectoid  $\text{Cu}_{41}\text{Sn}_{11}$  and a Cu–Sn solid solution can be seen in light blue, even when polished. The dark grey spots are  $\text{Cu}_2\text{S}$  (Fig. 5a–c). After etching with Klemm2, the colour changes to blue, the dendrites are red–dark blue or yellow–bright blue and the eutectoid areas are bright and encircled in dark blue (Fig. 5d–f).

In SEM, the bright eutectoid structure is clearly demarcated from the Cu–Sn solid solution, and some white Pb spots and dark  $\text{Cu}_2\text{S}$  patches are visible (Fig. 5g–i).

cc5 is quite different and contains 1.08 wt% As and 0.55 wt% S, but no Sn and only 0.07 wt% Pb (Table 1). The dendritic solidification structure is already visible in the polished sample and different coloured phases can be seen in the interdendritic areas (Fig. 6a–c). Copper is strongly coloured after etching, and the sulphides or arsenides are not attacked (Fig. 6d–f). In SEM,  $\text{Cu}_2\text{S}$  appears dark grey and the interdendritic areas with  $\text{Cu}_3\text{As}$  are bright grey (Fig. 6g–i).

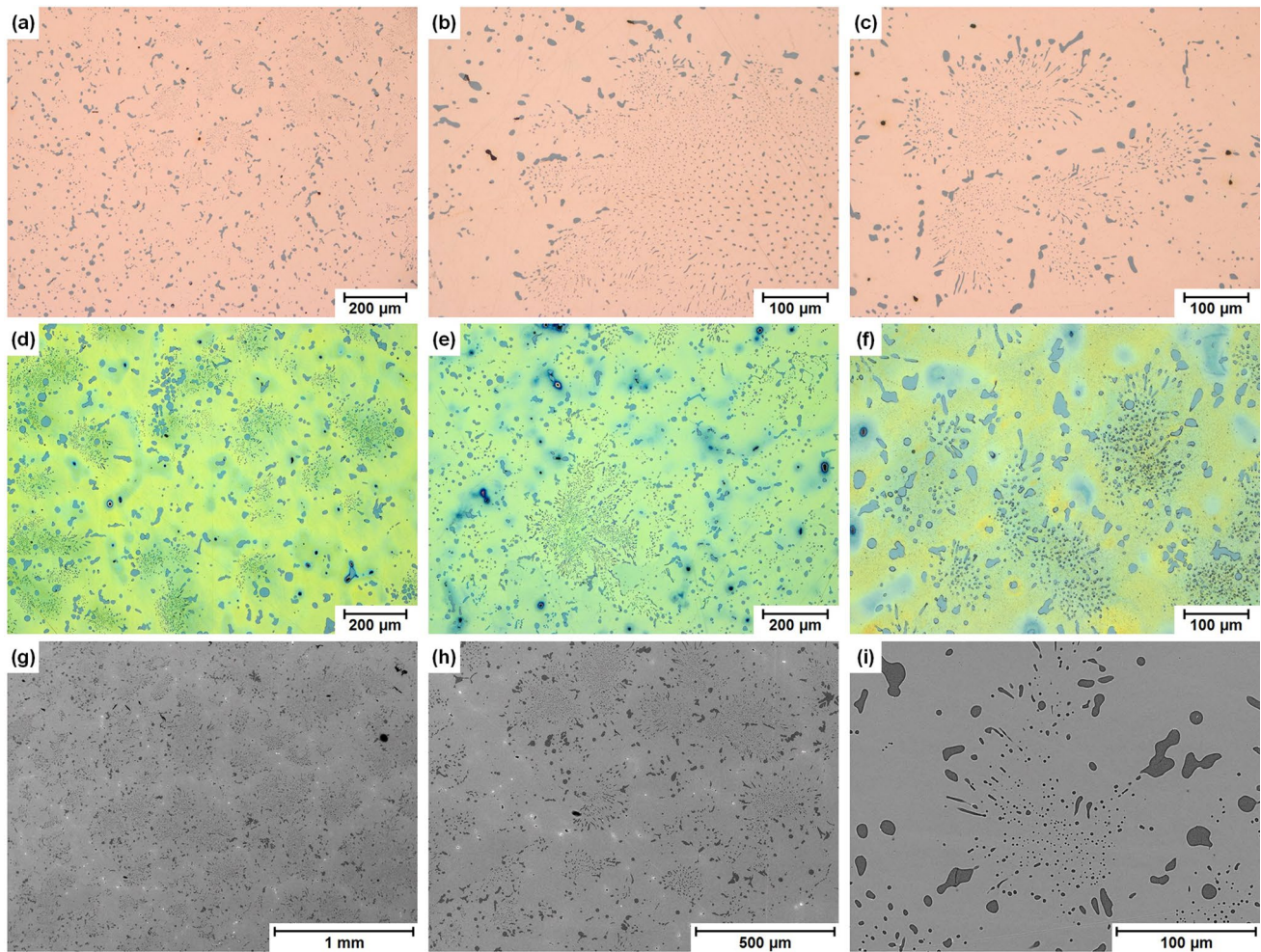


**Fig. 7** Metallography of cast cake cc6. **a–c** Polished sample, LOM, **d–f** Klemm2 etched, LOM, **g–i** SEM.

cc6 contains the least impurities with 0.32 wt% Pb and 0.51 wt% S, but no Sn or As (Table 1). A typical eutectic structure can already be seen on the polished sample, which can be described as a  $\text{Cu}_2\text{S}$ -Cu eutectic due to the present S content (Fig. 7a–c). After etching,  $\text{Cu}_2\text{S}$  appears darker and colour gradients can be seen in the Cu solid solution, which can be attributed to segregation effects during solidification (Fig. 7d–f). In SEM,  $\text{Cu}_2\text{S}$  is dark (Fig. 7g–i) and isolated white Pb spots are visible (Fig. 7h–c).

The casting cakes cc4, cc5 and cc6 are characterized by low Pb contents. However, they are very different regarding to their Sn and As contents. cc4 could be called tin bronze and cc5 arsenic bronze. In contrast, cc6 is almost pure Cu with a Cu–S eutectic. The different manufacturing methods of the various copper alloys will not be discussed here.

### The Fragments of Sickles and Socket Axe

The sickle is one of the oldest farming tools used to cut wild grain or grass and its use has been documented as early as the Neolithic [30]. After bronze was available and the casting process was mastered, bronze sickles have been documented since the Middle Bronze Age. Essentially a distinction is made between button sickles and tongue sickles, which were used in different ways in Europe [31, 32]. Since sickles break during use or errors occur during manufacture, it is not surprising that hoard finds contain sickles and their fragments (Fig. 8a–d). Three sickle fragments (si1, si2 and si3) could be examined, which consist of different composed tin bronzes (Table 1).

In the sickle fragment si1, 4.31 wt% Sn, 0.12 wt% S and 0.61 wt% Pb as well as 0.14 wt% As were measured





**Fig. 8** Examined sickle (si) fragments. **a** General view of a sickle (not examined), **b** si1, **c** si2, **d** si3.

(Table 1). The copper structure is homogeneous with isolated pores and fine precipitations with various impurities (S, Pb and As) (Fig. 9a). A structure with the intermetallic phase  $\text{Cu}_{41}\text{Sn}_{11}$ , which is often observed in Sn bronzes, is not present (Fig. 9b). The surface of the sickle is covered with a patina of malachite ( $\text{Cu}_2(\text{CO}_3)(\text{OH})_2$ ) and  $\text{Cu}_2\text{O}$  (Fig. 9b, c). In polarized light,  $\text{Cu}_2\text{O}$  (red) is mainly inside and malachite (green) at the rim of the corroded layer.

After etching, the dendritic solidification structure is clearly visible, which can be attributed to segregation effects by alloying elements in Cu (Fig. 9d). In polarized light, connected dendritic regions can be distinguished (Fig. 9e) and the dendritic patterns still can be seen in the corroded patina (Fig. 9f).

There are severely deformed areas near an edge (Fig. 9g–i), and at high magnification, the dendritic structures are cloudy and deformation lines in different directions are visible (Fig. 9i), i.e. this sickle area was subject of greater deformation forces during manufacture or use.

The sickle fragment si2 contains 10,06 wt% Sn, 0,31 wt% S, 0,79 wt% Pb and 0.15 wt% As (Table 1). Due to the high Sn content, the interdendritic areas are clearly distinguishable because the intermetallic, eutectoidic phase  $\text{Cu}_{41}\text{Sn}_{11}$  has been formed (Fig. 10a–c). Similar to sickle ss1, the dendritic areas are clearly visible in polarized light and after etching (Fig. 10d–g). In this sample, the dendritic solidification structures of the bronze can be seen well in the corroded patina (Fig. 10h–i).

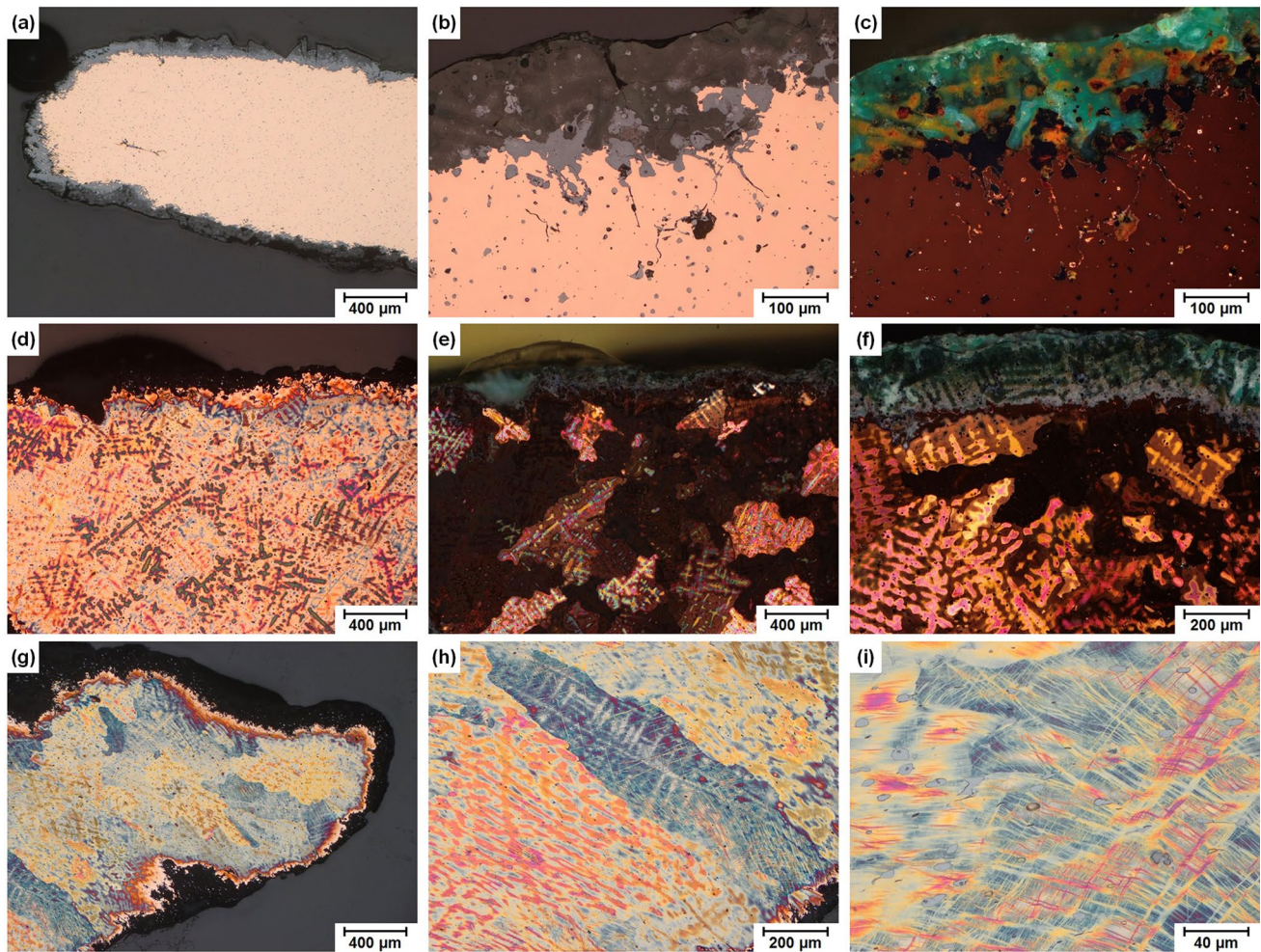


**Fig. 9** Metallography of sickle si1. **a–c** Polished sample, LOM, **(c, e, f)** polarized light, **(d–i)** Klemm2 etched.

Sickle fragment si3 contains 6,49 wt% Sn, 0,24 wt% S and 0,7 wt% Pb, but no As (Table 1). Some pores with a size of up to 2 mm can be seen in the overview micrograph (Fig. 11a) and a patina which entirely covers the surface. Various precipitates ( $\text{Cu}_2\text{S}$  and Pb) and the intermetallic, eutectoid phase already can be seen on the polished sample (Fig. 11b, c). In contrast to the other samples, it is noticeable that here the copper dendrites corrode preferentially, but not the interdendritic areas (Fig. 11d–g). Similar to si2, the  $\text{Cu}_{41}\text{Sn}_{11}$  phase remains in the corrosion layer.

Again, deformed dendrites at the sickle's tip were observed (Fig. 11d, e).

A SEM–EDX element distribution shows that Cl and Sn are enriched in the dendritic corrosion products (Fig. 12). Sn enrichment in the patina is specific for Sn bronzes [27, 33, 34].

The socket axe was developed in the Middle Bronze Age and often exhibits various decorative elements, which were already present in the mould (Fig. 13a, b) [35]. The axes were fixed on an angled wooden shaft and used as a tool or weapon [36]. A fragment of a socket axe from the Drassburg hoard was examined (Fig. 13c, d).

The socket axe fragment sa1 contains 4,47 wt% Sn, 2,54 wt% Pb, 0.14 wt% As and only 0,08 wt% S (Table 1). The copper matrix contains many spherical pores with diameters of up to 200  $\mu\text{m}$  (Fig. 14a, b). This indicates poor copper processing and poor casting conditions. In the polished state, the usual precipitations of a low-alloyed bronze can be seen in the structure ( $\text{Cu}_2\text{S}$ , Pb and  $\text{Cu}_{41}\text{Sn}_{11}$ ) (Fig. 14c). The etched structure shows strong colour differences, but not well-developed dendrites—maybe a combination of contamination and poor casting conditions (Fig. 14d). Again, the

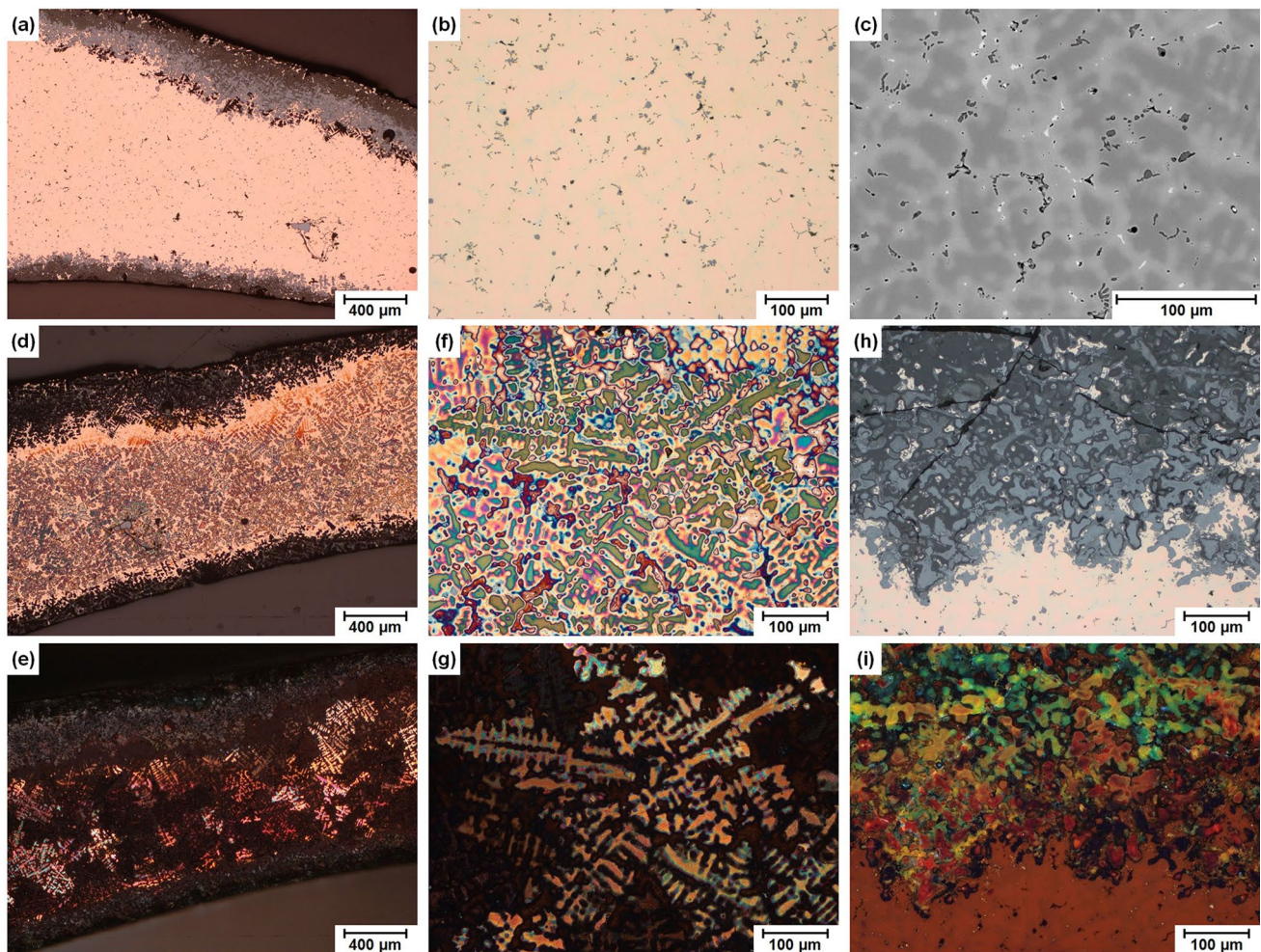


**Fig. 10** Metallography of sickle si2. (a, b, h, i) Polished sample, LOM (c) SEM, (d–g) Klemm2 etched, LOM, (e, g, i) polarized light.

patina on the bronze surface contains malachite and  $\text{Cu}_2\text{O}$  (Fig. 14e, f).

## Conclusions

Ten copper samples from the Drassburg hoard were examined by metallography.

It can be assumed that the cast cakes were the starting material for the production of objects using the casting process. Since the composition of the individual cast cakes is quite different, it can be assumed that most of them do not come from primary copper production.

Cast cake cc6 contains only small amounts of Pb and some S, indicating a manufacture from chalcopyrite. For cc5, fahlore could be assumed to be the used copper ore, because of the raised As content. cc4 consists of Sn bronze

and was either made from raw materials or was produced by co-melting of bronze and recycled material.

In the casting cakes cc1, cc2 and cc3, the high Pb content indicates that Pb or Pb ores were intentionally added to the copper.

The sickles and a socket axe fragments consist of Sn bronze with different contents of Sn, Pb, As and S. The sickle fragments have dendritic solidification and some deformation structures. The socket axe has increased porosity, which ultimately results in poor material properties.

Reflections about recycling of copper in the Bronze Age: If one considers the hoard find from Drassburg is a material deposit of a Bronze Age smelter or blacksmith, it means that it is impossible to trace the copper ore sources using Pb isotopy or trace element analysis. On the one hand, this

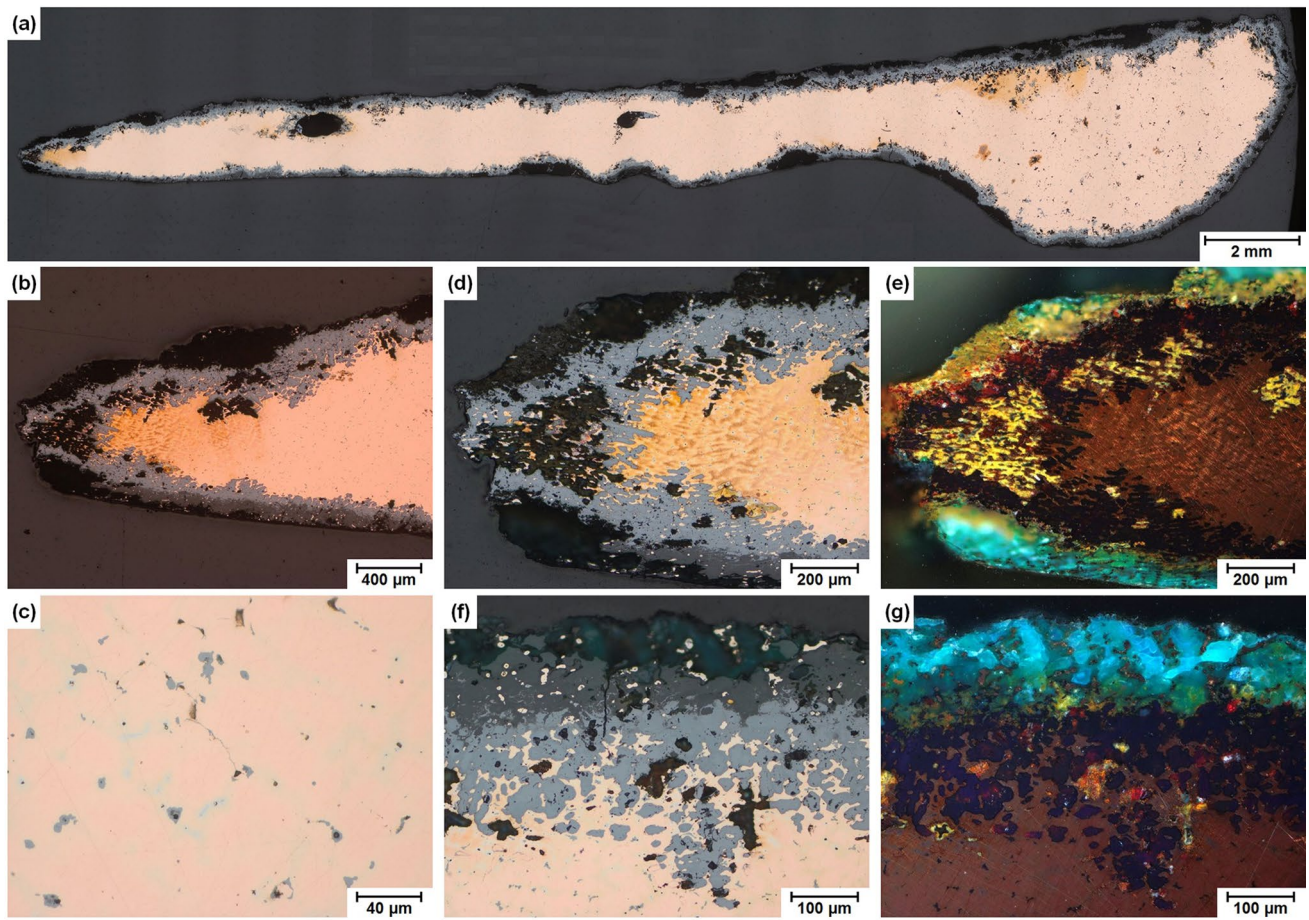


**Fig. 11** Metallography of sickle si3. (a–g) Polished sample, LOM, (e, g) polarized light.

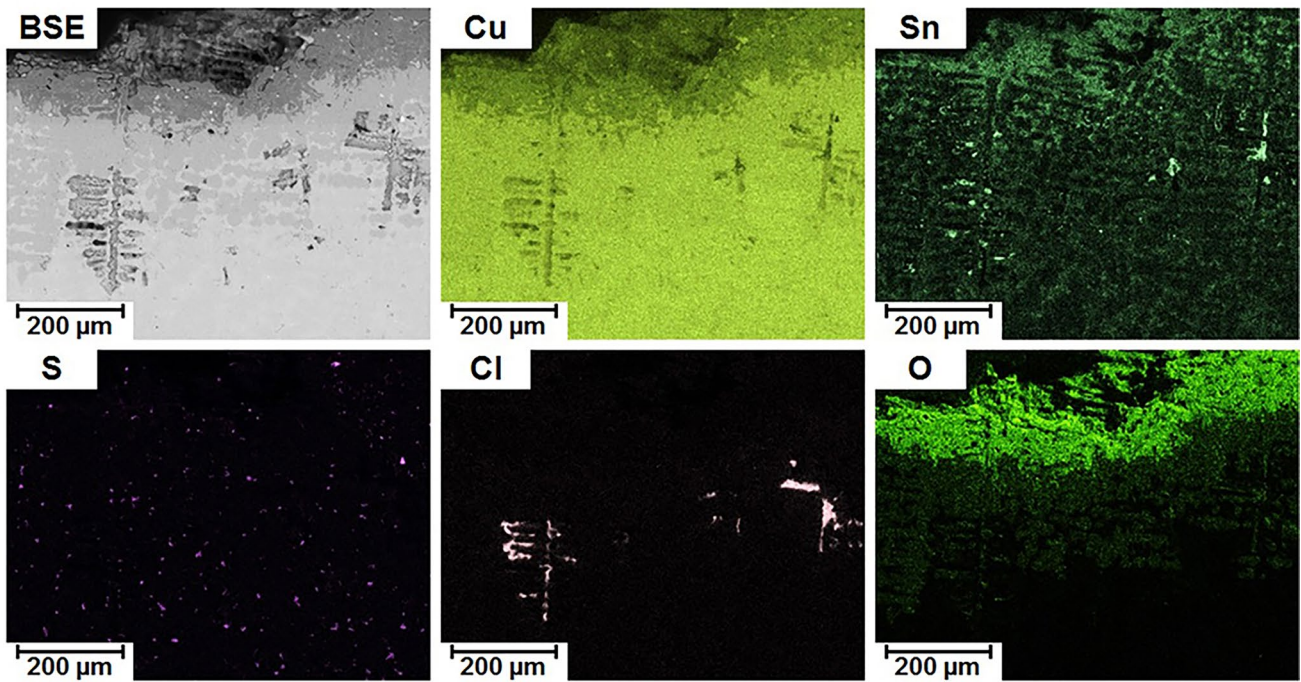
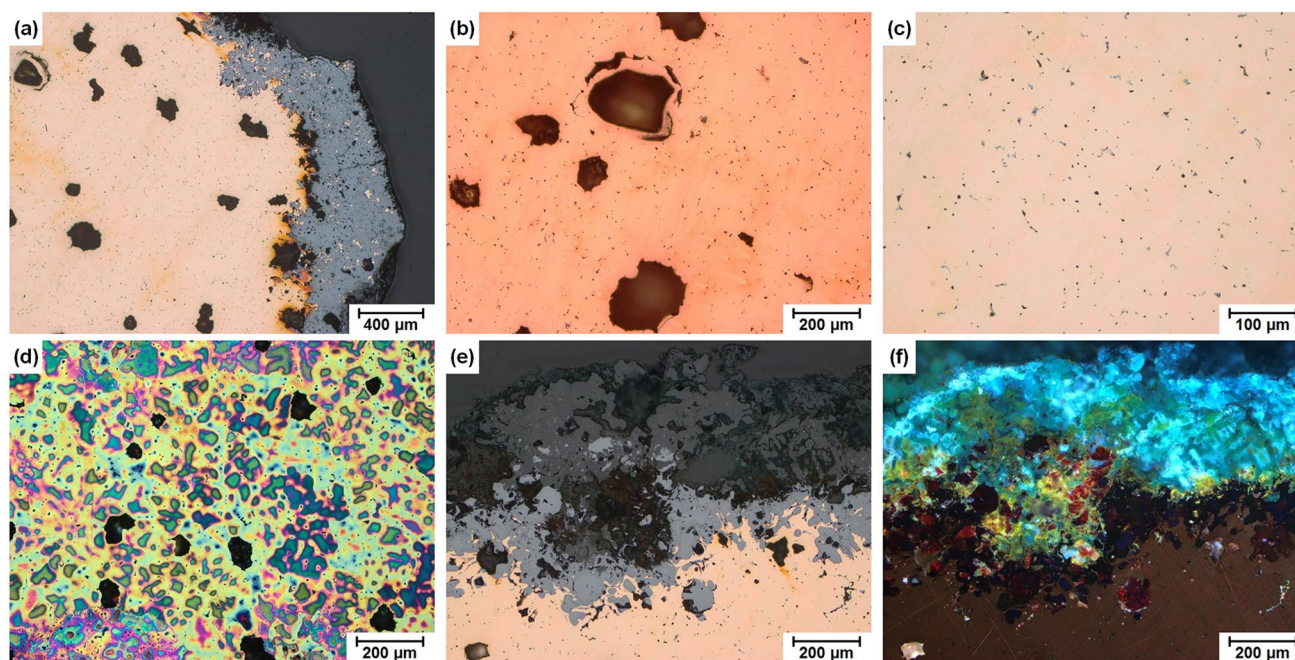


Fig. 12 SEM–EDX element distribution of sickle si3.



Fig. 13 Examined spout axe (sa). (a, b) Overall view of a whole socket axe (not examined), (c, d) section photographed from two directions.



**Fig. 14** Metallography of socket axe sa1. (a–c, e, f) Polished sample, LOM, (d) Klemm2 etched, LOM, (e, f) corroded edge, (f) polarized light.

applies to the presented copper alloys on the other hand for objects made from recycled material.

**Acknowledgements** Our thanks go to Dr. Hannes Herdits from Burgenländische Landesmuseen in Eisenstadt for providing the samples. We would also like to thank Mr. Marton Ritter and Mr. Philipp Burski, who helped with the sample preparation for their bachelor thesis.

**Funding** Open access funding provided by TU Wien (TUW).

**Open Access** This article is licensed under a Creative Commons Attribution 4.0 International License, which permits use, sharing, adaptation, distribution and reproduction in any medium or format, as long as you give appropriate credit to the original author(s) and the source, provide a link to the Creative Commons licence, and indicate if changes were made. The images or other third party material in this article are included in the article's Creative Commons licence, unless indicated otherwise in a credit line to the material. If material is not included in the article's Creative Commons licence and your intended use is not permitted by statutory regulation or exceeds the permitted use, you will need to obtain permission directly from the copyright holder. To view a copy of this licence, visit <http://creativecommons.org/licenses/by/4.0/>.

## References

- H. Herdits, Bemerkungen zur Metallurgie bronzezeitlicher Depotfunde. *Burgenländische Heimatblätter*. **67**, 100–104 (2005)
- T. Vachta, *Bronzezeitliche Hortfunde und ihre Fundorte in Böhmen*, *Berlin studies of the ancient world* 33 (Edition Topoi, Berlin, 2016)
- V. Kiss, K.P. Fischl, G. Kulcsar, *Chronology of the Early and Middle Bronze Age in Hungary. New results*, *STUDIA HERCYNIA* XXIII/2, 173–197 (2019)
- M.K.H. Eggert, S. Samida, *Ur- und Frühgeschichtliche Archäologie*, UTB basics, UTB GmbH, 2nd Ed. (2009)
- A. Ballmer, Zur Topografie des bronzezeitlichen Deponierens. Von der Handlungstheorie zur Raumanalyse, *Prähistorische Zeitschrift*. **85**, 120–131 (2010)
- S. Hansen, Über bronzezeitliche Depots, Horte und Einzel funde: Brauchen wir neue Begriffe? *Archäologische Informationen*. **25**, 91–97 (2002)
- S. Hansen, *Hillforts and Weaponry in the Early and Middle Bronze Age*, in: S. Hansen/R. Krause (eds.), *Materialisierung von Konflikten. Materialisation of Conflict. Prähistorische Konfliktforschung* (Bonn 2019), **4**, 93–132 (2020)
- O. Dietrich, Learning from ‘scrap’ about Late Bronze Age hoarding practices A biographical approach to individual acts of dedication in large metal hoards. *Eur. J. Archaeol.* **17**, 468–486 (2014)
- S. Honti, K. Jankovits, The warrior aristocracy of the Late Bronze Age Urnfield Period in County Somogy, south-western Transdanubia. The Lengyeltóti V hoard (County Somogy/Hungary). *Acta Archaeologica Academiae Scientiarum Hungaricae*. **73**, 143–162 (2022)
- T. Vachta, *Bronzezeitliche Hortfunde und ihre Fundorte in Böhmen*, *Berlin studies of the ancient world*; 33 (Excellence Cluster Topoi, Berlin, 2016)
- D. Rožnovský, *Der Hortfund aus der späten Bronzezeit aus Mikulovice (Bez. Znojmo)*, in: A. Kozubová, E. Makarová, M. Neumann (eds.): *Slovenská archeológia. Ultra velum temporis. Venované Jozefovi Bátorovi k 70. narodeninám*, 527–535 (2020)
- A. Krenn-Lieb, *Ressource versus Ritual – Deponierungsstrategien der Frühbronzezeit in Österreich*, In: H. Meller, F. Bertemes (Hrsg.), *Der Griff nach den Sternen. Tagungen des Landesmuseums für Vorgeschichte Halle/Saale Band 05*, 281–315 (2010)
- M. Windholz-Konrad, *Urnenfelderzeitliche Mehrstückhorte aus dem Salzkammergut zwischen Ödensee und Hallstättersee*, *Österreichische Denkmaltopographie* 2 (2018) Bundesdenkmalamt, Vienna

14. R.F. Tylecote, H.A. Ghaznavi, P.J. Boydell, Partitioning of Trace Elements between the Ores, Fluxes, Slags and Metal during the Smelting of Copper. *J. Archaeol. Sci.* **4**, 305–333 (1977)
15. R.F. Tylecote, *Summary of results of experimental work on early copper smelting*, in: *Aspects of Early Metallurgy* (Oddy W. A. Ed.). London: British Museum, pp. 5–12 (1980)
16. R.F. Tylecote, *The Early History of Metallurgy*, London–New York (1987)
17. A.M. Pollard, P. Bray, A. Cuénod, P. Hommel, Y.-K. Hsu, R. Liu, L. Perucchetti, J. Pouncett, M. Saunders, *Beyond Provenance: New Approaches to Interpreting the Chemistry of Archaeological Copper Alloys*, in: *Studies in Archaeological Sciences*, Leuven University Press (2018)
18. R.F. Tylecote, *A history of metallurgy* (The Metals Society, Mid County Press London, 1976)
19. R. Haubner, Die prähistorische Kupfermetallurgie – allgemeine Betrachtungen. *BHM Berg- Huettenmaenn. Monatsh.* **166**, 343–351 (2021)
20. R. Haubner, S. Strobl, P. Trebsche, *Metallographic analyses from the late Urnfield period copper mining settlement at Prigglitz-Gasteil in Lower Austria*, in: R. Turck, T. Stöllner and G. Goldenberg (Eds), *Alpine Copper II – Alpenkupfer II – Rame delle Alpi II – Cuivre des Alpes II. New Results and Perspectives on Prehistoric Copper Production*, Der Anschnitt, Beiheft 42, (2019), Verlag Marie Leidorf, Bochum. pp. 323–332
21. H. Herdits, *Die ostalpine bronzezeitliche Kupfererzeugung im überregionalen Vergleich am Grundbeispiel eines Hüttenplatzes in Mühlbach/Sbg.*, Doctoral Thesis at University Vienna, Vienna (2017)
22. F. Ertl, S. Strobl, R. Haubner, An ancient bronze ingot smelted from fahllore. *Mater. Sci. Forum.* **891**, 613–617 (2017)
23. R. Haubner, F. Ertl, S. Strobl, Examinations of a Bronze Ingot Made of Fahllore. *Practical Metallography.* **54**, 107–117 (2017)
24. R. Haubner, S. Strobl, M. Thurner, H. Herdits, Ein Kupfergusskuchen mit hohem Antimonengehalt aus Velem/Westungarn. *BHM Berg- Huettenmaenn. Monatsh.* **165**, 453–460 (2020)
25. D. Modl, Zur Herstellung und Zerkleinerung von plankonvexen Gusskuchen in der spätbronzezeitlichen Steiermark. Österreich, Experimentelle Archäologie in Europa. **9**, 127–152 (2010)
26. I. Baranyi, Betrachtungen über die Herkunft des Zinns in der Bronzezeit. *Carolinea.* **58**, 115–124 (2000)
27. R. Haubner, S. Strobl, P. Trebsche, Analysis of Urnfield period bronze droplets formed during casting. *Mater. Sci. Forum.* **891**, 41–48 (2017)
28. E. Pernicka, J. Lutz, T. Stöllner, *Bronze age copper produced at Mitterberg, Austria, and its distribution*, *Archaeologia. Austriaca.* **100**, 19–55 (2016)
29. T.K. Waldner, M. Mehofer, M. Bode, Prehistoric slags and ores from the Vinschgau – Geochemical and archaeometallurgical analyses. *Geo. Alp.* **17**, 5–18 (2021)
30. M.R. Behm-Blancke, J. Boese, *Zu spätchalkolithischen Erntegeräten in Nordsyrien und Südostanatolien*. in: R.M. Boehmer and J. Maran (Hrsg.), *Lux Orientis. Archäologie zwischen Asien und Europa. Festschrift für Harald Hauptmann zum 65. Geburtstag*. Rahden, Leidorf 27–37 (2001)
31. E. Fejér, Bronze age sickles in diverse roles. *Hungarian Archaeology.* **9**, 23–30 (2020)
32. S. Arnoldussen, H. Steegstra, A bronze harvest: Dutch Bronze Age sickles in their European context. *Palaeohistoria.* **57(58)**, 63–109 (2016)
33. R. Haubner, S. Strobl, *Long-time corrosion of a cast bronze droplet during 3000 years storage in soil*, in: *Proceedings EURO-CORR 2015*, Paper-Nr. **116**, 1–6 (2015)
34. R. Haubner, S. Strobl, M. Thurner, H. Herdits, Ein bronzenes Griffzungenmesser aus dem Burgenland. *BHM Berg- Huettenmaenn. Monatsh.* **166**, 352–357 (2021)
35. K. Kippert, *Die Äxte und Beile im mittleren Westdeutschland II (Prähistorische Bronzefunde)* C.H.Beck, München (1984)
36. P. Trebsche, Ein Tüllenbeil mit Resten der Holzschäftung und weitere bronzezeitliche Funde aus Enns. *Archäologie Österreichs.* **13(1)**, 40–43 (2002)

**Publisher's Note** Springer Nature remains neutral with regard to jurisdictional claims in published maps and institutional affiliations.